Computation of Singular Posture of New 15-DOF Anthropomorphic Robotic Fingers

Deepak Bharadwaj[#], Roushan Kumar

Department of Mechanical Engineering, School of Engineering, University of Petroleum and Energy Studies, Dehradun, India
***[#]Corresponding Author:** Deepak Bharadwaj, Email: dbharadwaj@ddn.upes.ac.in*

Abstract

A new finger gripper design had been proposed in the present work. The existing design of finger gripper has limitations in manipulability. Earlier the tension wire and pulley system has been used for the finger gripper movement. Due to that, the load-carrying capacity of the finger gripper is very low. The proposed design has a combination of serial linkage and parallel linkages. Each finger has 3-DOF. The four fingers of the gripper are attached to the common shaft, and the joint was actuated by one flat plate EC motor. The last finger is attached separately to the shaft and each joint was actuated separately. The dimension of the finger gripper is kept approximately to the anthropomorphic finger. Jacobian and singularity postures were computed for different orientations.

Keywords: Finger Gripper, linkages, Singularity, Posture, Anthropomorphic.

1. INTRODUCTION

The robotic finger gripper design can increase the dexterity and manipulability of the robotic hand. A proper design of a robotic finger can easily grasp the object and avoid collision between the fingers. The automation of a multi-finger robotic end effector plays a crucial role in agile manufacturing for grasping objects [1]. The recent trends have changed in finger gripper design. In place of rigid finger gripper, the research community focus on flexible soft robotic grippers [2]. The soft robotic gripper can easily manipulate the object in an unknown environment [3].

The EMG control interfaces closely interact with the object and perform the task. Multi-finger joint control is an issue. A single actuator control differential mechanism is used to operate the closing and opening of the fingers. Soft robotics emerges in clinical operations as an alternative for therapeutic abilities [4]. A single actuator Differential mechanisms reduced the actuator requirement and possess convenient grasps [5],[6]. The help of a flexible roller chain and simple mechanism allow the finger gripper to grasp a big object. The tendon movement and elastic force of the spring help the finger to open and close very easily. 3- D printed robotic finger was fused with the thermoplastic polyurethane. The fused soft robotic finger has pneumatic sensing chambers. The control of finger force, as well as position, was achieved with the help of a pneumatic sensing chamber. The biomimetic and biomechanics properties were implemented in a new robotic finger gripper. The robotic finger gripper was actuated using five pneumatic cylinders. The motion is obtained similarly to the human upper limb finger. The efficacy were obtained 0.93 i.e closer to the human finger movement [7].

Soft and actuate robotic finger gripper has an advantage over rigid finger gripper. The compliance feature of the soft gripper has a broad range of object manipulability [8],[9]. Controlling the multi-finger robotic gripper is a tedious task. The grasping force of the finger with an object depends on the hemispherical fingertip radius of contact. In the biomimetic finger gripper. Muscle force and moments were tendon driven and match with human finger capability [10]. Generally, lightweight materials like

elastomer material were used for developing the finger gripper. Elasto materials are lightweight and durable and very easy to maintain [11].

The proposed research work was carried out for the combination of serial and parallel multi-finger joint actuation. The development of a flat plate EC brushless DC motor enables to actuation of the finger joint individually. The flat plate DC motor size was varying from 6mm -19mm in diameter and the length is varying from 10-20mm. The finger length is kept the same approximately to the anthropomorphic finger. There is no motion between the crossed fingers. The combination of the serial and parallel finger increases the manipulability of grasping the object and load carrying capacity also increased.

2. CONCEPTUAL DESIGN AND MODELLING

The design was developed in the Solid Work software. Each finger has three parts. The first part of the finger is named as finger base. The center distance between the two ends of the finger base is 37.5 mm and 15mm in width. The detail of the finger base is shown in figure 1. An assembly has been developed by adding the EC flat motor and shaft. The first part of the finger is connected to the palm. The base of all the finger base parts is concentric. The shaft is inserted in the hole, i.e. also concentric to the base part. Each finger is bolted on the shaft so that each finger move simultaneously. The flat plate motor is supported on the palm and drives the shaft, so that the finger base part has the same motion. The finger's second part is also connected in the same way. The EC flat motor is supported on the finger base part and drives the shaft. During motion, all the second parts of the finger move simultaneously and there is no collision between the first part and the second part. The last part of the finger is also connected in the same fashion. The fifth finger i,e thumb is connected in the same way, but actuation is done with the help of three individual flat plates EC motors [12]. A 3-D model of robotic fingers were shown in figure 1.

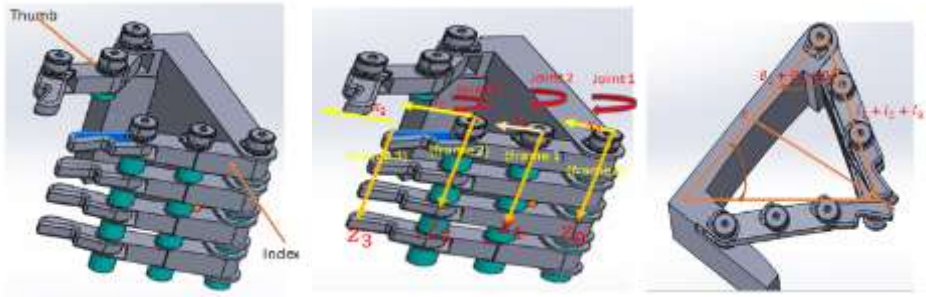

Fig. 1 a) 3-D view of robotic Fingers b) Joint-link description c) Collision detection

2.1. **Forward & Inverse Kinematics**

The kinematic model describes the finger movement in space. Each finger has 3-DOF. All the joints are revolute and active joints. The four fingers of the gripper has the same orientation and moved in the same plane. Each of the four fingers is separated by a distance of 10mm. So there is no collision occurs in the crossed finger position, because the mechanical configuration of the finger does not allow it to move in another direction. The fifth finger has the same orientation but rotates in the opposite direction so that it can grasp the object. Each finger can be modelled as a kinematic chain with three links connected by the three joints [13]. The Denaavit-Hartenberg method was adopted for finding the workspace of the finger. The workspace of all the fingers is the same. The joint notation scheme and complete frame assignment are shown in figure 1 a, 1b, and 1c and joint link parameter for the finger gripper are determined and tabulated in table 1.

Table 1. Joint link parameter for the finger gripper

Link	Parameters 1 (θ_i)	Joint parameters (d_i)	Parameters 2 (l_i)	Parameters 3 (a_i)
	θ_1	0	l_1	0
	θ_2	0	l_2	0
	θ_3	0	0	0

Where θ_i is a rotation about Z_{i-1} axis,d_i is the translation along Z_{i-1} axis, a_i is the translation by a distance along x_i axis,α_i is the rotation about x_i axis. The workspace of index finger 1 is evaluated as follows

$$ {}^0_3T = {}^0_1T * {}^1_2T * {}^2_3T \quad (1) $$

=

$$ \begin{bmatrix} \cos(\theta_1+\theta_2+\theta_3) & -\sin(\theta_1+\theta_2+\theta_3) & 0 & l_2\cos(\theta_1+\theta_2)+l_1\cos(\theta_1)+l_3\cos(\theta_1+\theta_2+\theta_3) \\ \sin(\theta_1+\theta_2+\theta_3) & \cos(\theta_1+\theta_2+\theta_3) & 0 & l_2\sin(\theta_1+\theta_2)+l_1\sin(\theta_1)+l_3\sin(\theta_1+\theta_2+\theta_3) \\ 0 & 0 & 1 & 0 \\ 0 & 0 & 0 & 1 \end{bmatrix} $$

Similarly, the workspace of the other finger was evaluated. The joint displacements$(\theta_1, \theta_2, \theta_3)$ that lead the finger gripper to a certain position and orientation T can be found by solving the kinematic model equations for unknown joint displacements. The close-form solution was obtained for different values of finger joint with equations (1) to (5).

$$ \theta_2 = \cos^{-1}\frac{(d_x-l_3n_x)^2+(d_y-l_3n_y)^2-{l_2}^2-{l_1}^2}{2l_1l_2} \quad (2) $$

$$ \theta_1 = \varphi - \psi + \cos^{-1} C \quad (3) $$

Where $\varphi = \theta_1+\theta_2+\theta_3 = \tan^{-1}\frac{n_y}{n_x} + 180° \quad (4)$

$\psi = \tan^{-1}\frac{B}{A}$,

$x = {d_x}^2 + {d_y}^2 - {l_2}^2 - {l_1}^2 - {l_3}^2 - 2l_1l_2\cos(\theta_2)$.

$A = 2l_1l_3 + 2l_3l_2 * u$, $B = 2l_3l_2 * v$

$u = \cos(\theta_2)$, $v = \sin(\theta_2)$,

$C = \frac{x}{\sqrt{A^2+B^2}}$

$$ \theta_3 = \tan^{-1}\frac{n_y}{n_x} + 180° - \theta_2 - \theta_1 \quad (5) $$

2.2 Jacobian & Singular Posture

The finger movement depends on the finger joint velocities. The Jacobian describes the finger joint position with respect to time. The Jacobian relates the joint velocity of the finger to the end finger velocity. The closing and opening of the gripper depend on the Jacobian matrix[14]. The Jacobian matrix for the first finger is computed as follows with equations (6) and (7).

$$ J(q) = [J_1 \quad J_2 \quad J_3] \quad (6) $$

Where

$$J_1 = \begin{bmatrix} -l_2 \sin(\theta_1 + \theta_2) - l_1 \sin(\theta_1) - l_3 \sin(\theta_1 + \theta_2 + \theta_3) \\ l_2 \cos(\theta_1 + \theta_2) + l_1 \cos(\theta_1) \\ 0 \\ 0 \\ 0 \\ 1 \end{bmatrix}$$

$$,J_2 = \begin{bmatrix} -l_2 \sin(\theta_1 + \theta_2) - l_3 \sin(\theta_1 + \theta_2 + \theta_3) \\ l_2 \cos(\theta_1 + \theta_2) + l_3 \cos(\theta_1 + \theta_2 + \theta_3) \\ 0 \\ 0 \\ 0 \\ 1 \end{bmatrix}, J_3 = \begin{bmatrix} -l_3 \sin(\theta_1 + \theta_2 + \theta_3) \\ l_3 \cos(\theta_1 + \theta_2 + \theta_3) \\ 0 \\ 0 \\ 0 \\ 1 \end{bmatrix}$$

The loss of motion of the finger will start at the point from where the finger is coming into contact with the other finger. Since there is no lateral degree of freedom, due to other finger is not affecting the motion of the other finger. But possibility occurs at the point from where the thumb finger is coming into contact with the index finger. Two types of singularity were computed. The interior singularities were occurs when the tip of the finger is located inside the reachable workspace of the finger gripper. These are caused when two or more joint axes become collinear and at a specific end-effector configuration [15]. The computational of internal singularities can be carried out by analyzing the rank of the Jacobian matrix[16]- [22]. The Jacobian matrix loses its rank and becomes vanishes [23]-[27], that is $\det|J| = 0$. This is computed by portioning the Jacobian matrix into three $2X2$ submatrices.

$$J_1 = \begin{bmatrix} -l_2 \sin(\theta_1 + \theta_2) - l_1 \sin(\theta_1) - l_3 \sin(\theta_1 + \theta_2 + \theta_3) & -l_2 \sin(\theta_1 + \theta_2) - l_3 \sin(\theta_1 + \theta_2 + \theta_3) \\ l_2 \cos(\theta_1 + \theta_2) + l_1 \cos(\theta_1) + l_3 \cos(\theta_1 + \theta_2 + \theta_3) & l_2 \cos(\theta_1 + \theta_2) + l_3 \cos(\theta_1 + \theta_2 + \theta_3) \end{bmatrix}$$

$$J_2 = \begin{bmatrix} -l_2 \sin(\theta_1 + \theta_2) - l_3 \sin(\theta_1 + \theta_2 + \theta_3) & -l_3 \sin(\theta_1 + \theta_2 + \theta_3) \\ l_2 \cos(\theta_1 + \theta_2) + l_3 \cos(\theta_1 + \theta_2 + \theta_3) & -l_3 \cos(\theta_1 + \theta_2 + \theta_3) \end{bmatrix} \quad (7)$$

$$J_3 = \begin{bmatrix} -l_2 \sin(\theta_1 + \theta_2) - l_1 \sin(\theta_1) - l_3 \sin(\theta_1 + \theta_2 + \theta_3) & -l_3 \sin(\theta_1 + \theta_2 + \theta_3) \\ l_2 \cos(\theta_1 + \theta_2) + l_1 \cos(\theta_1) + l_3 \cos(\theta_1 + \theta_2 + \theta_3) & -l_3 \cos(\theta_1 + \theta_2 + \theta_3) \end{bmatrix}$$

From expression (7), the interior singular position was obtained by solving the expression

$$\det|J_1| = l_1 l_2 \sin(\theta_2) + l_1 l_3 \sin(\theta_2 + \theta_3) = 0 \quad (8)$$

$$\det|J_2| = l_2 l_3 \sin(\theta_3) = 0 \quad (9)$$

$$\det|J_3| = l_2 l_3 \sin(\theta_3) + l_1 l_3 \sin(\theta_2 + \theta_3) = 0 \quad (10)$$

Since the thumb finger and index finger i.e. finger1 and finger2 are parallel in orientation. During grasping, both fingers made contact at three points. Condition 1 occurs at the point where both finger 1 and finger 2 comes in contact. Condition 1 is shown in figure 2. These points were computed by the expression (7) to (11).

$$\theta_1 + \theta_2 + \theta_3 = \sin^{-1} \frac{x}{2(l_1 + l_2 + l_3)} \quad (11)$$

3. RESULTS

The first singularity posture was obtained at $\theta_3 = 0° \; and \; 180°$, the second singularity posture was obtained at $\theta_2 = 0° \; and - 180°$. The actuation constraint does not allow the $\theta_1$to rotate more than

90°. Singular postures were obtained at a different computed angle. Figures 2 and 3 show the simulated result of singular posture.

Fig. 2. Singular posture of the fingers including thumb finger and index finger

Fig. 3. Collision detection in all the fingers

4. CONCLUSION

The robotic finger gripper design has been considered for the grasping of the object. : A new finger gripper design had been proposed in the present work. The propped design can actuate the four joints of the finger simultaneously. The other two joints of the finger have also actuated with the help of a flat plate EC motor. The index finger was actuated separately. Singularities were computed for the different angles. A collision-free movement of the gripper was observed during the operation.

REFERENCES

[1] M. Honarpardaz, M. Tarkian, J. Ölvander, and X. Feng, "Finger design automation for industrial robot grippers: A review," *Rob. Auton. Syst.*, vol. 87, pp. 104–119, 2017, doi: 10.1016/j.robot.2016.10.003.

[2] Z. Chen, H. Rahimi Nohooji, and C.-M. Chew, "Development of Topology Optimized Bending-Twisting Soft Finger," *J. Mech. Robot.*, vol. 14, no. 5, Feb. 2022, doi: 10.1115/1.4053159.

[3] M. Liu, L. Hao, W. Zhang, and Z. Zhao, "A novel design of shape-memory alloy-based soft robotic gripper with variable stiffness," *Int. J. Adv. Robot. Syst.*, vol. 17, no. 1, pp. 1–12, 2020, doi: 10.1177/1729881420907813.

[4] M. Zhu, M. Xie, X. Lu, S. Okada, and S. Kawamura, "A soft robotic finger with self-powered triboelectric curvature sensor based on multi-material 3D printing," *Nano Energy*, vol. 73, no. March, p. 104772, 2020, doi: 10.1016/j.nanoen.2020.104772.

[5] J. Zhou, J. Yi, X. Chen, Z. Liu, and Z. Wang, "BCL-13: A 13-DOF soft robotic hand for dexterous grasping and in-hand manipulation," *IEEE Robot. Autom. Lett.*, vol. 3, no. 4, pp. 3379–3386, 2018, doi: 10.1109/LRA.2018.2851360.

[6] R. Kumar, N. J. Ahuja, M. Saxena, and A. Kumar, "Automotive Power Window Communication with DTC Algorithm and Hardware-in-the Loop Testing," Wirel. Pers. Commun., 2020;114 (4): 3351–3366 doi: 10.1007/s11277-020-07535-4.

[7] C. Gosselin, F. Pelletier, and T. Laliberté, "An anthropomorphic underactuated robotic hand with 15 dofs and a single actuator," *Proc. - IEEE Int. Conf. Robot. Autom.*, pp. 749–754, 2008, doi: 10.1109/ROBOT.2008.4543295.

[8] R. Kumar, K. Bansal, A. Kumar, J. Yadav, M. K. Gupta, and V. K. Singh, "Renewable energy adoption: Design, development, and assessment of solar tree for the mountainous region," Int. J. Energy Res. 2021; 1–17 doi: 10.1002/er.7197.

[9] Gupta V., Kumar R., Mishra R.G., Semwal A., Siwach S., "Design and optimization of luggage tracking system on airport", Proceeding of International Conference on Intelligent Communication, Control and Devices Advances in Intelligent Systems and Computing (2016), pp. 833-838.
[10] C. Y. Chu and R. M. Patterson, "Soft robotic devices for hand rehabilitation and assistance: A narrative review," *J. Neuroeng. Rehabil.*, vol. 15, no. 1, pp. 1–14, 2018, doi: 10.1186/s12984-018-0350-6.
[11] K. Xu and H. Liu, "Continuum Differential Mechanisms and Their Applications in Gripper Designs," *IEEE Trans. Robot.*, vol. 32, no. 3, pp. 754–762, 2016, doi: 10.1109/TRO.2016.2561295.
[12] R. Kumar, Divyanshu, and A. Kumar, "Nature Based Self-Learning Mechanism and Simulation of Automatic Control Smart Hybrid Antilock Braking System," Wirel. Pers. Commun., 2021; 116(4); 3291–3308.
[13] S. E. Baek, S. H. Lee, and J. H. Chang, "Design and control of a robotic finger for prosthetic hands," *IEEE Int. Conf. Intell. Robot. Syst.*, vol. 1, pp. 113–117, 1999, doi: 10.1109/iros.1999.812990.
[14] C. Tawk, H. Zhou, E. Sariyildiz, M. In Het Panhuis, G. M. Spinks, and G. Alici, "Design, Modeling, and Control of a 3D Printed Monolithic Soft Robotic Finger with Embedded Pneumatic Sensing Chambers," *IEEE/ASME Trans. Mechatronics*, vol. 26, no. 2, pp. 876–887, 2021, doi: 10.1109/TMECH.2020.3009365.
[15] Y. Mishima and R. Ozawa, "Design of a robotic finger using series gear chain mechanisms," *IEEE Int. Conf. Intell. Robot. Syst.*, vol. 1, no. IROS, pp. 2898–2903, 2014, doi: 10.1109/IROS.2014.6942961.
[16] Kumar, R., Kumar, A., Gupta, M. K., Yadav, J., & Jain, A. (2022). Solar tree-based water pumping for assured irrigation in sustainable Indian agriculture environment. Sustainable Production and Consumption, 33, 15-27, doi.org/10.1016/j.spc.2022.06.013.
[17] Kumar, R., Kumar, A., Gupta, M. K., Yadav, J., & Jain, A. (2022). Solar tree-based water pumping for assured irrigation in sustainable Indian agriculture environment. Sustainable Production and Consumption, 33, 15-27, doi.org/10.1016/j.spc.2022.06.013.
[18] B. S. Homberg, R. K. Katzschmann, M. R. Dogar, and D. Rus, "Haptic identification of objects using a modular soft robotic gripper," *IEEE Int. Conf. Intell. Robot. Syst.*, vol. 2015-Decem, pp. 1698–1705, 2015, doi: 10.1109/IROS.2015.7353596.
[19] D. Chadefaux, J. L. Le Carrou, M. A. Vitrani, S. Billout, and L. Quartier, "Harp plucking robotic finger," *IEEE Int. Conf. Intell. Robot. Syst.*, pp. 4886–4891, 2012, doi: 10.1109/IROS.2012.6385720.
[20] R. Kumar, R. K. Pachauri, P. Badoni, D. Bharadwaj, U. Mittal, and A. Bisht, "Investigation on parallel hybrid electric bicycle along with issuer management system for mountainous region," J. Clean. Prod., 2022; 362:132430, doi: 10.1016/j.jclepro.2022.132430.
[21] Kumar, R., Gupta, N., Bharadwaj, D., Dutt, D., & Joshi, A. (2022). Design and development of electronic clutch control unit for manual transmission. Materials Today: Proceedings.
[22] Kumar, R., Gupta, M. K., Kumar, A., Sharma, P., & Deorari, R. (2022). Analysis of electronic clutch control unit for manual transmission vehicle oriented toward safety. Materials Today: Proceedings.
[23] Maan A., Pitta P., Yadav J. (2018) Performance Evaluation of Rectangular Fins by Modeling and Simulations. In: Siddiqui N., Tauseef S., Abbasi S., Rangwala A. (eds) Advances in Fire and Process Safety. Springer Transactions in Civil and Environmental Engineering. Springer, Singapore.
[24] Yadav J., Agnihotri G. (2018) Circumvention of Friction-Induced Stick-Slip Vibration by Modeling and Simulation. In: Singh R., Choudhury S., Gehlot A. (eds) Intelligent Communication, Control and Devices. Advances in Intelligent Systems and Computing, vol 624. Springer, Singapore.
[25] Jitendra Yadav and Geeta Agnihotri (2017), "Modeling and Simulation of the Dynamic Response of a Generic Mechanical Linkage for Control Application Under the Consideration of Nonlinearities Imposed by Friction", In Springer Proceedings of the International Conference on Nano-electronics, Circuits & Communication Systems, Lecture Notes in Electrical Engineering 403, DOI 10.1007/978-981-10-2999-8_26
[26] Jitendra Yadav & G. Agnihotri, "Proposed Critical Damping for a Spring Mass System to Avoid Stick Slip" ,Springer Journal of the institution of engineers (India): Series C Volume 96, Number 3, PP 331-335, July-September 2015. https://doi.org/10.1007/s40032-015-0173-1
[27] Yadav, Jitendra, et al. "Nonlinear dynamics of controlled release mechanism under boundary friction." Results in Engineering 11 (2021): https://doi.org/10.1016/j.rineng.2021.100265